ISSN 0006-3509, Biophysics, 2010, Vol. 55, No. 4, pp. 592–599. © Pleiades Publishing, Inc., 2010.
Original Russian Text © A.Yu. Buchin, A.V. Chizhov, 2010, published in Biofizika, 2010, Vol. 55, No. 4, pp. 664–673.

CELL BIOPHYSICS

Firing-Rate Model of a Population of Adaptive Neurons

A. Yu. Buchin and A. V. Chizhov

Ioffe Physical-Technical Institute, Russian Academy of Sciences, St. Petersburg, 194021 Russia
E-mail: Anton.Chizhov@mail.ioffe.ru

Received July 9, 2008; in final form, April 13, 2010

Abstract—A firing rate (FR) model for a population of adaptive leaky integrate-and-fire neurons has been proposed. Unlike known FR models, it describes more precisely the unsteady firing regimes and takes into account the effect of slow potassium currents of spike adaptation. Approximations of the adaptive channel conductances are rewritten from voltage-dependent to spike-dependent and then to rate-dependent ones. The proposed FR model is compared with a very detailed population model, namely, the conductance-based Refractory Density model. This comparison shows the coincidence of the first peak of activity after the start of stimulation as well as of the stationary state. As an example of simulation of coupled adaptive neuronal populations, a ring model has been constructed, which reproduces a visual illusion known as tilt after-effect. The FR model is recommended for mathematical analysis of neuronal population activity as well as for computationally expensive large-scale network simulations.

Keywords: neuronal population model, firing-rate model, spike adaptation, integrate-and-fire neuron, kinetics of adaptive currents, tilt after-effect

DOI: 10.1134/S0006350910040135

INTRODUCTION

Large-scale mathematical models of the nervous system or its separate structures often describe the interaction not of single neurons (or not only single neurons) but neuronal populations, i.e. large groups of cells of the same type receiving similar input synaptic signals. Such models are based on single-population models where the input consists of synaptic currents and conductances, and the output characteristic is the rate of neuronal pulses (spikes) averaged over the set of neurons constituting the population. Just as in proceeding from the description of separate particles to macroscopic description of ensembles in statistical physics, the population equations are derived from single-neuron equations but differ from them essentially. If the equations of the dependence of the population firing rate on the input characteristics are algebraic relationships or ordinary differential equations (ODEs), such a model is conventionally called a Firing-Rate (FR) model, as distinct from other more complex population models. Most of the FR models calculate the population neuron spike rate either by the averaged input current or by the population-averaged subthreshold potential, with the rate vs. current (potential) dependence (often S-shaped) reflecting the steady-state behavior of a single neuron [1–3]. Rate smoothing in transition regimes is achieved by writing a relaxation ODE with an artificial relaxation time parameter and a sigmoid function as a source [1], or a second-order ODE with an additional rate parameter [2].

FR models only approximately describe the dynamics of population activity. In the general case, it is important how the neurons are distributed in respect of the phases of their spike activity. Neuronal synchronization and desynchronization may substantially alter the evolution of the population rate even at a relatively constant firing rate. Such activity can be reproduced with the aid of the probability density approach, which considers the evolution of neuronal state distribution density. Population models based on simplified models of single neurons and developed in this approach have been proposed [4–7] and comprehensively discussed [8, 9]. For detailed neuron models with a large set of ion channels of the Hodgkin–Huxley (HH) type, including slow channels of spike adaptation, a population model has been constructed [10–12] and called conductance-based Refractory Density model (RD). Although quite precise models are available for populations of simplified and of biophysically detailed neurons, still topical is construction of simple FR models that provide for quick computation and are readily amenable to mathematical analysis. Therewith they must be more or less capable of describing nonstationary regimes.

If neurons of a uniform population receiving a common stimulus start to fire, their first spikes prove

Abbreviations: (A)LIF, (adaptive) leaky integrate-and-fire; HH, Hodgkin–Huxley; FR, firing-rate; RD, refractory density (model).

to be almost synchronous, forming a "volley." Such a population response may have dominant influence on the neurons that receive synaptic signals from this population. It is for this reason that FR models must reproduce the burst-like neuronal population activity. Another weighty cause of the change in the firing rate of realistic neurons is the effect of slow ion channels resulting in spike adaptation, a gradual change of the interspike intervals under a constant synaptic input. Therefore, the FR model must allow for the shunting and hyperpolarizing action of the input synaptic conductances and currents, respectively. To this end, the population model—just as the neuron model—must contain two control signal parameters, i.e., must retain the cardinal property of the neuron [13]. All these requirements are met by the model proposed here. We consider a population of simple but realistic adaptive leaky integrate-and-fire (ALIF) neurons, and build an FR model, using the RD model as a reference. This is a generalization of the earlier model for a population of non-adaptive LIF neurons [14].

Inclusion of adaptive currents into consideration introduces certain difficulties associated with that the initial approximations are voltage-dependent, i.e. depend on the spike shape, which is not computed in FR models. However, for an HH-type neuron (p. 1.1) the adaptive currents can be roughly taken to depend only on the moments of firing, being almost independent of the potential between spikes [15]. Thus we can make spike-dependent approximations of adaptive channel conductances and thereby generalize the model of a single LIF neuron (p. 1.2) for the case of spike adaptation (p. 1.3). Further we proceed to rate-dependent approximations (p. 1.5) of adaptive channels suitable for an FR model. For the population of ALIF neurons defined in p. 1.4, we briefly present the RD model (p. 1.6) and offer a new FR model (p. 1.7). We test the quality of approximations by comparing the proposed FR model with the RD reference (p. 2.1). Upon discussing the results we conclude that the proposed model can be expediently used in large-scale simulation of brain activity.

1. MODEL DESCRIPTION

1.1. Hodgkin–Huxley neuron equations. We start from the model of a rat hippocampus CA1 pyramidal cell [11], which itself was a simplification of the model [16] built on experimental data. The model includes the following voltage-dependent ion currents: sodium $I_{Na}(t, V)$, fast potassium $I_K(t, V)$, leakage $I_L(t, V) = g_L(V - V_L)$; and potassium $I_M(t, V)$, $I_{AHP}(t, V)$ with respective characteristic action times of 10 and 100 ms providing for spike adaptation. Below, $V(t)$ is membrane potential; V_{Na}, V_K, V_{AHP}, V_M denote current reversal potentials of the respective channels; g_L is leakage conductance, V_L is leakage current reversal potential; $\bar{g}_{Na}$, $\bar{g}_K$, $\bar{g}_{AHP}$, $\bar{g}_M$ are maximal conductances; $I(t)$ is input or synaptic current measured at a fixed potential V_L; $g_S(t)$ is input or synaptic conductance. The equations have the form

$$C\frac{dV}{dt} = -I_{Na} - I_K - I_{AHP} - I_M - g_L(V - V_L) + I - g_S(V - V_L), \quad (1)$$

$$I_{Na} = \bar{g}_{Na}x_{Na}(t)(V - V_{Na}), \quad (2)$$

$$I_K = \bar{g}_K x^4(t)y^3(t)(V - V_K), \quad (3)$$

$$I_{AHP} = \bar{g}_{AHP}w(t)(V - V_{AHP}), \quad (4)$$

$$I_M = \bar{g}_M n^2(t)(V - V_M). \quad (5)$$

The dependences of ion channel conductance on the potential are expressed through dimensionless conductances $x_{Na}(t, V)$, $x(t, V)$, $y(t, V)$, $w(t, V)$, $n(t, V)$ [11]. For adaptive currents, the channel kinetics write down as

$$\frac{dw}{dt} = \frac{w_\infty(V) - w}{\tau_{AHP}(V)}, \quad (7)$$

$$w_\infty = 1/(1 + \exp(-(V + 35)/10)), \quad (8)$$

$$\tau_{AHP} = 2000/3.3\exp((V + 35)/20) + \exp(-(V + 35)/10)\ \text{ms}, \quad (9)$$

$$\frac{dn}{dt} = \frac{n_\infty(V) - n}{\tau_M(V)}, \quad (10)$$

$$n_\infty(V) = \frac{a(V)}{a(V) + b(V)}, \quad (11)$$

$$\tau_M(V) = \frac{1}{a(V) + b(V)} + 8\ \text{ms}, \quad (12)$$

$$a(V) = 0.003\exp(0.135(V + 45))\ \text{ms}^{-1}, \quad (13)$$

$$b(V) = 0.003\exp(-0.090(V + 45))\ \text{ms}^{-1}. \quad (14)$$

The time profiles of voltage-dependent conductances of the M- and AHP channels and the potential are displayed in Fig. 1 (a, c, e).

1.2. LIF neuron equations. The model of a leaky integrate-and-fire neuron consists of the potential equation including only the leakage and the synaptic currents, and the threshold (fire-and-reset) condition (after V exceeds V^T, it drops to V_{reset}, each such event making a spike):

$$C\frac{dV}{dt} = -g_L(V - V_L) + I - g_S(V - V_L), \quad (15)$$

$$\text{if } V > V^T, \text{ then } V = V_{reset}. \quad (16)$$

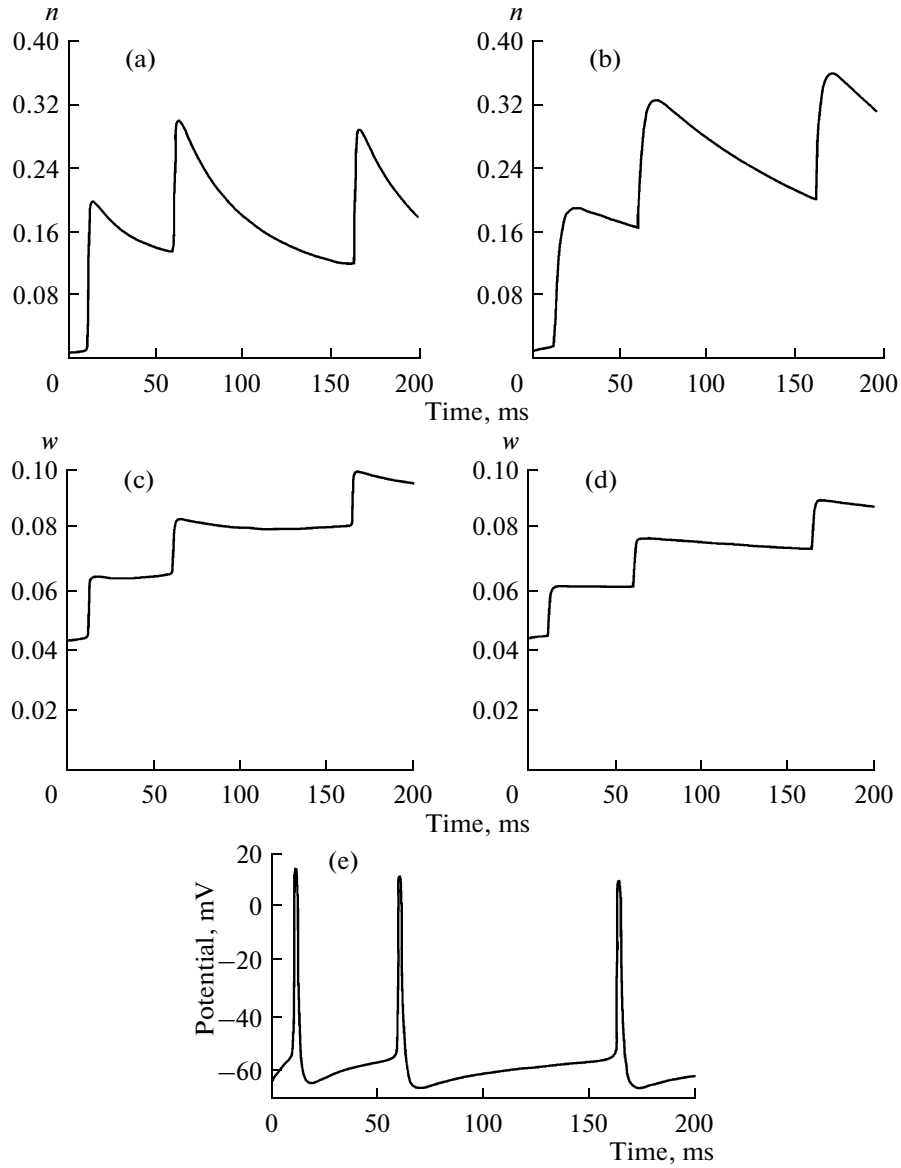

Fig. 1. Dimensionless conductances of the M- and AHP channels (a, c) and potential (e) of an adaptive HH-type neuron calculated with equations (1)–(14) at $I = 500$ pA, and the corresponding dimensionless conductances (b, d) in the spike-dependent approximations (17), (18).

Figure 2 collates the behavior of a non-adaptive HH-type and an LIF neuron. It is evident that at appropriately chosen V^{T} and V_{reset} the firing moments agree reasonably, and the interspike potentials are roughly commensurate. Thus, the described reduction can be used to reproduce the spiking patterns of neuronal activity.

1.3. Spike-dependent approximations for adaptive conductances. Most neurons have slow channels for spike adaptation. In the model based on equations (1)–(14), adaptive currents can be provisionally divided into a faster M current and slower AHP current. These currents must be included into the LIF models, which requires changing the approximations since the integrate-and-fire and the HH potentials differ greatly, especially during the spikes.

Figure 1 panels (a) and (c) show the dynamics of M- and AHP-channel conductances calculated in the HH model (1)–(14). One can see rapid increments at every spike, with smooth relaxation to the $n_\infty(V_{\mathrm{L}})$ and $w_\infty(V_{\mathrm{L}})$ values, i.e., weak voltage dependence between the spikes. Therefore we can pass from voltage-dependent approximations to spike-dependent ones. The kinetics of opening of the channels controlled by spikes (delta-functions) is defined by time constants τ^1_{AHP}, τ^1_{M}, and the closure kinetics, by τ^0_{AHP}, τ^0_{M}. The equations for spike-dependent approximations of

dimensionless conductances of adaptive currents are second-order ODEs:

$$\tau^1_{\rm AHP}\tau^0_{\rm AHP}\frac{d^2w}{dt^2} + (\tau^1_{\rm AHP} + \tau^0_{\rm AHP})\frac{dw}{dt} - w_\infty + w = \frac{\chi(1-w)}{K(1/\tau^1_{\rm AHP}, 1/\tau^0_{\rm AHP})}\sum_i \delta_i(t - t_{\rm spike}), \quad (17)$$

$$\tau^1_{\rm M}\tau^0_{\rm M}\frac{d^2n}{dt^2} + (\tau^1_{\rm M} + \tau^0_{\rm M})\frac{dn}{dt} - n_\infty + n = \frac{\xi(1-n)}{K(1/\tau^1_{\rm M}, 1/\tau^0_{\rm M})}\sum_i \delta_i(t - t_{\rm spike}), \quad (18)$$

where

$$K(a, b) = \frac{ab}{a-b}\left\{\left(\frac{a}{b}\right)^{b/(b-a)} - \left(\frac{a}{b}\right)^{a/(b-a)}\right\}.$$

Here $\delta(t - t_{\rm spike})$ is a Dirac delta-function corresponding to a spike occurring at $t_{\rm spike}$. The approximation parameters $w^0_\infty = 0.058$, $n^0_\infty = 0.082$ correspond to $w_\infty(V_{\rm L})$, $n_\infty(V_{\rm L})$, while $\tau^0_{\rm AHP} = 414$ ms, $\tau^0_{\rm M} = 124$ ms, $\tau^1_{\rm AHP} = 1$ ms, $\tau^1_{\rm M} = 3$ ms, $\chi = 0.018$, $\xi = 0.175$ were chosen such that the conductance increments at the spike and the characteristic times of conductance rise and drop would be roughly equal for voltage-dependent and spike-dependent approximations. The $K(a, b)$ normalization is necessary for the conductance increments at spikes to be explicitly given by χ and ξ.

Figure 1 panels (b) and (d) show the dynamics of M- and AHP-channel conductances calculated in the spike-dependent approximation. One can see not only qualitative but even good quantitative agreement with the calculations in the full HH model (panels (a) and (c) respectively). This means that we can use the spike-dependent approximations for an LIF neuron.

1.4. Population of adaptive (ALIF) neurons. We consider a neuronal population as an infinite set of similar neurons receiving common input current I and conductance $g_{\rm s}$ but individual noise with dispersion σ_I. Each neuron in the framework of the ALIF model is described by equations (15), (16) with $I_{\rm M}$, $I_{\rm AHP}$ and a noise component of input current [11]:

$$C\frac{dV}{dt} = -(g_{\rm L} + g_{\rm S})(V - V_{\rm L}) - \bar{g}_{\rm M}n^2(t)(V - V_{\rm L}) - \bar{g}_{\rm AHP}w(t)(V - V_{\rm AHP}) + I + \sigma_I\xi(t), \quad (19)$$

if $V > V^{\rm T}$, then $V = V_{\rm reset}$.

Conductances w and n are calculated with (17)–(19), white noise $\xi(t)$ corresponds to conditions $\langle\xi(t)\rangle = 0$, $\langle\xi(t)\xi(t')\rangle = \tau^0_{\rm m}\delta(t - t')$, where $\tau^0_{\rm m} = C/g_{\rm L}$ is the time constant of membrane at rest. The noise amplitude determines the steady-state potential dispersion $\sigma_V = \sqrt{2}\,\sigma_I/g_{\rm tot}$. The full membrane conductance $g_{\rm tot} = \bar{g}_{\rm AHP}w(t) + \bar{g}_{\rm M}n^2(t) + g_{\rm L} + g_{\rm s}$; $\tau_{\rm m} = C/g_{\rm tot}$ is the effective time constant of the neuronal membrane.

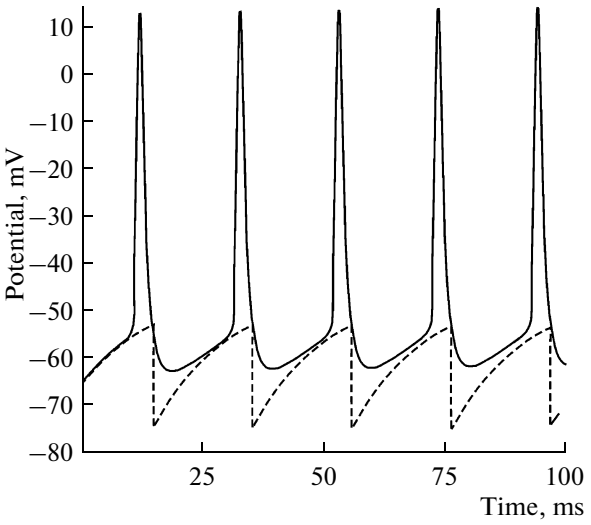

Fig. 2. Activity of an LIF neuron (dashed line) and an HH-type neuron without adaptive currents (solid line).

To obtain the population firing rate $\nu(t)$, we first consider a large enough set of neurons described by (19); the number of spikes occurring in each small time interval, $n_{\rm act}(t; t + \Delta t)$, is divided by the neuron number N and by Δt. Then we formally proceed to infinite N and infinitesimal Δt. The resulting rate describes the population activity:

$$\nu(t) = \lim_{\Delta t \to 0}\lim_{N \to \infty}\frac{1}{\Delta t}\frac{n_{\rm act}(t; t + \Delta t)}{N}. \quad (20)$$

Note that in the above definition, the response of a neuronal population is equivalent to an aggregate of responses of a single neuron with various noise realizations. Direct Monte Carlo simulations are restricted to a finite number of neurons (realizations), which results in approximate calculation of $\nu(t)$.

1.5. Rate-dependent approximations for adaptive currents. To build the FR model, we need the conductances for the AHP and M currents controlled by the spike rate $\nu(t)$. In the given case we average the approximations (17), (18) over multiple neurons (realizations) as in transition from single spikes to the rate, and obtain

$$\tau^1_{\rm AHP}\tau^0_{\rm AHP}\frac{d^2w}{dt^2} + (\tau^1_{\rm AHP} + \tau^0_{\rm AHP})\frac{dw}{dt} - w_\infty + w = \frac{\chi(1-w)}{K(1/\tau^1_{\rm AHP}, 1/\tau^0_{\rm AHP})}\nu(t), \quad (21)$$

$$\tau_M^1\tau_M^0\frac{d^2n}{dt^2} + (\tau_M^1 + \tau_M^0)\frac{dn}{dt} - n_\infty + n = \frac{\xi(1-n)}{K(1/\tau_M^1, 1/\tau_M^0)}\nu(t). \quad (22)$$

All numerical values of the coefficients are the same as in (17), (18).

1.6. Refractory Density model of a population of ALIF neurons. An efficient way of describing a population of HH-type neurons is the RD model, derived and tested previously [10–12]. The population is regarded as a continuum of neurons distributed in a one-dimensional space of parameter t^*, the time elapsed since the last spike, which characterizes the state of refractoriness between spikes and thus the readiness of a neuron to fire again. The distribution of neurons in the t^* space is characterized by density $\rho(t, t^*)$, and their state, by realization-average potential $U(t, t^*)$ and mean ion channel conductances, which are also parameterized via t^*. Formally, the parameterization boils down to replacing the full time derivatives with a sum of partial derivatives: $d/dt = \partial/\partial t + \partial/\partial t^*$. The set of consistent equations for these dependent variables is governed by the input synaptic current $I(t)$ and conductance $g_S(t)$, and allows calculating the population neuron firing rate $\nu(t)$. This approach can almost exactly reproduce the behavior of a population modeled as a large number of HH-type neurons. Here we apply it to adaptive neurons. The RD population model written out for ALIF neurons is:

$$\frac{\partial\rho}{\partial t} + \frac{\partial\rho}{\partial t^*} = -\rho H, \quad (23)$$

$$C\left(\frac{\partial U}{\partial t} + \frac{\partial U}{\partial t^*}\right) = (-(g_L + g_S))(U - V_L) - \bar{g}_M n^2(t)(U - V_M) - \bar{g}_{AHP} w(t)(U - V_{AHP}) + I, \quad (24)$$

$$\frac{\partial n}{\partial t} + \frac{\partial n}{\partial t^*} = \frac{n_\infty(U) - w}{\tau_M(U)}, \quad (25)$$

$$\frac{\partial w}{\partial t} + \frac{\partial w}{\partial t^*} = \frac{w_\infty(U) - w}{\tau_{AHP}(U)}, \quad (26)$$

$$\nu(t) = \rho(t, 0) = \int_{+0}^{\infty}\rho H dt^*, \quad (27)$$

$$U(t, 0) = V_{reset}. \quad (28)$$

Here n_∞, τ_M, w_∞, τ_{AHP} are defined by (8), (9), (11)–(14); H characterizes the probability of one neuron firing (hazard function). Together with the dynamic threshold $U^T(dU/dt)$ it determines the action of sodium currents and noise. The H function has been approximated [12] as

$$H(U(t, t^*)) = \frac{1}{\tau_m}(A(U) + B(U, dU/dt)), \quad (29)$$

$$\tau_m = C/g_{tot}, \quad \sigma_V = \sqrt{2}\sigma_I/g_{tot}, \quad g_{tot} = \bar{g}_{AHP} w(t, t^*) + \bar{g}_M n^2(t, t^*) + g_L + g_S(t), \quad (30)$$

$$T = (U^T - U)/\sqrt{2}\sigma_V, \quad (31)$$

$$A(U) = \exp(6.1\times10^{-3} - 1.12T - 0.257T^2 - 0.072T^3 - 0.0117T^4), \quad (32)$$

$$B(U, dU/dt) = -\frac{2}{\sqrt{\pi}}\tau_m\left[\frac{dT}{dt}\right]\frac{\exp(-T^2)}{1 + erf(T)}, \quad (33)$$

where $[f]_+ = f$ if $f > 0$ and zero otherwise. The two summands in H both estimate the probability of a neuron potential reaching the threshold but pertain to different processes: $B(U)$, to raising the mean potential; $A(U)$, to potential dispersal by noise.

1.7. The FR model for a population of ALIF neurons. The analogy in building RD and FR models has been shown elsewhere [14]. Here we propose to generalize the FR model for neurons with adaptation. FR models do not distinguish neurons by their state between spikes, but we can suppose that the potential magnitudes are distributed randomly about the mean $U(t)$ in accordance with the input noise. The mean membrane potential is determined by an ODE averaging (19):

$$C\frac{dU}{dt} = -(g_L + g_S)(U - V_L) - \bar{g}_M n^2(t)(U - V_M) - \bar{g}_{AHP} w(t)(U - V_{AHP}) + I. \quad (34)$$

The population firing rate is set by an analog of H, namely:

$$\nu(t) = \bar{A}(U) + \bar{B}(U, dU/dt), \quad (35)$$

$$\bar{A}(U) = \left(\tau_m\sqrt{\pi}\int_{(V_{reset} - U)/\sigma_V\sqrt{2}}^{(V^T - U)/\sigma_V\sqrt{2}} e^{u^2}(1 + erf(u))du\right)^{-1}, \quad (36)$$

$$\bar{B}(U, dU/dt) = \frac{1}{\sqrt{2\pi}\sigma_V}\left[\frac{dU}{dt}\right]_+\exp\left(-\frac{(V_T - U)^2}{2\sigma_V^2}\right), \quad (37)$$

where

$$\tau_m = C/g_{tot}, \quad \sigma_V = \sqrt{2}\sigma_I/g_{tot}, \quad g_{tot} = \bar{g}_{AHP} w(t) + \bar{g}_M n^2(t) + g_L + g_S(t).$$

Here $\bar{A}(U)$ is the steady-state rate (expression first presented in [17] and quoted in [8]); $\bar{B}(U, dU/dt)$ is the rate in a nonstationary regime, the expression fol-

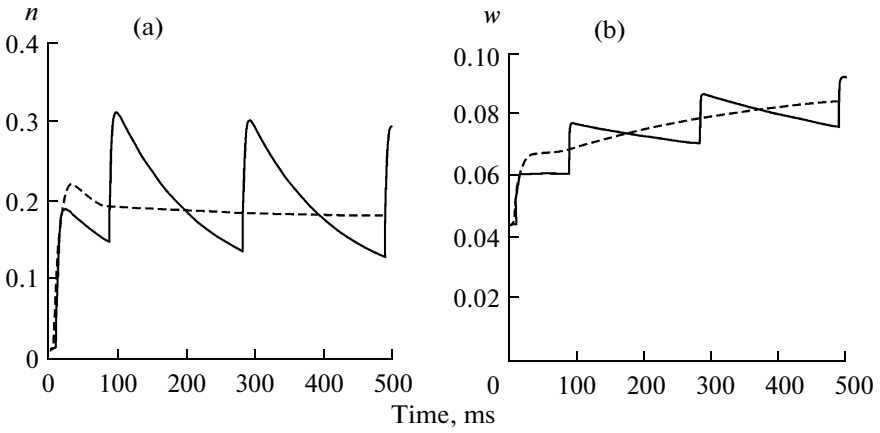

Fig. 3. Rate-dependent conductances of the M- and AHP-channels in the FR model (dashed lines) and spike-dependent conductances for a single ALIF neuron (solid lines).

lows from considering a Gaussian distribution of potentials about the mean $U(t)$ upon exceeding the V^{T} threshold. As above, $w(t)$, $n(t)$ are calculated from (21), (22).

Numerical parameter values: $w_\infty^0 = 0.058$, $\tau_{\mathrm{AHP}}^0 = 414$ ms, $\tau_{\mathrm{AHP}}^1 = 1$ ms, $\chi = 0.018$; $n_\infty^0 = 0.082$, $\tau_{\mathrm{M}}^0 = 124$ ms, $\tau_{\mathrm{M}}^1 = 3$ ms, $\xi = 0.175$; $V_{\mathrm{rest}} = -65.7$ mV, $V_{\mathrm{reset}} = -75.1$ mV; initial steady-state potential dispersion $\sigma_V = 2$ mV, i.e. $\sigma_I = (2\ \mathrm{mV})\, g_{\mathrm{L}}\sqrt{2}$; $V^{\mathrm{T}} = 10$ mV, $\bar{g}_{\mathrm{AHP}} = 0.6$ mS/cm^2, $\bar{g}_{\mathrm{M}} = 0.76$ mS/cm^2, $\tau_{\mathrm{m}}^0 = 14.4$ ms, $C = 1\ \mu$F/cm^2, $g_{\mathrm{L}} = C/\tau_{\mathrm{m}}^0$, $V_{\mathrm{M}} = -80$ mV, $V_{\mathrm{AHP}} = -70$ mV, $g_{\mathrm{S}} = 0$.

2. RESULTS

2.1. Testing the FR Population Model; Comparison with the RD Model. First, compare the dynamics of adaptive channel conductances $n(t)$ and $w(t)$ in a single ALIF neuron modeled with equations (17)–(19) and in the FR population model (34)–(37), (21), (22), upon stimulation with an $I = 500$ pA step. Figure 3 shows that the rate-dependent conductance is an adequate time averaging of the spike-dependent one. At the onset of stimulation the conductances rise sharply, and then tend to a limit determined by the steady-state firing rate.

Next, compare the population rate $\nu(t)$ plots for an ALIF neuron population obtained in the generalized FR model (34)–(37), (21), (22) and in the RD model (23)–(33), (8), (9), (11)–(14) at different combinations of input current I and noise amplitude σ_V (Fig. 4). We see that in all cases the main peak, corresponding to the first spikes of the population neurons directly upon stimulation, is adequately reproduced by the FR model with AHP- and M-currents. Further we see a gradual transition to a steady state, where the rates in the two models coincide. The FR model gives a rough approximation for the firing rate in the transition regime, almost without oscillations; the nonstationary term $\bar{B}$ of (35) is progressively nullified, and at large times (~1000 ms) there remains only $\bar{A}$ that determines the steady-state rate. The duration of the transition apparently depends on the noise amplitude.

Thus, both in the volley and in the steady state, at different stimulating currents and different extent of neuronal desynchronization by noise, the FR model agrees nicely with the reference RD model.

2.2. FR Modeling of Tilt After-Effect in a Neuronal Ring. Finally, we present an example of applying the FR model to interconnected populations. Consider a ring of coupled FR-populations that, similarly to [18], reproduces the selectivity of visual-cortex neurons with regard to the spatial orientation of a line stimulus. Generalizing then such a model for adaptive neurons, we may be able to simulate a psychophysical phenomenon known as the tilt after-effect [19].

We take the FR model of one (i-th) population based on equations (34)–(37), (22) at $g_{\mathrm{S}} = 0$ and $\bar{g}_{\mathrm{AHP}} = 0$ as the operator of transducing input current $I_i(t)$ into rate $\nu_i(t)$. Then we evenly arrange N populations on a ring, with angular coordinates $\theta_i = -\pi/2 + \pi i/N$ ranging from $-\pi/2$ to $\pi/2$. The synaptic current that couples the populations in the ring, according to [18], we write down as

$$I_i = N^{-1}\sum_{j=1}^{N}(J_0 + J_1\cos(\theta_i - \theta_j))\nu_j + I_0 + I_1\cos(\theta_i - \theta_0),$$

where I_0, I_1, J_0, J_1 are coupling parameters, θ_0 is the orientation of the stimulus. To simulate the illusion,

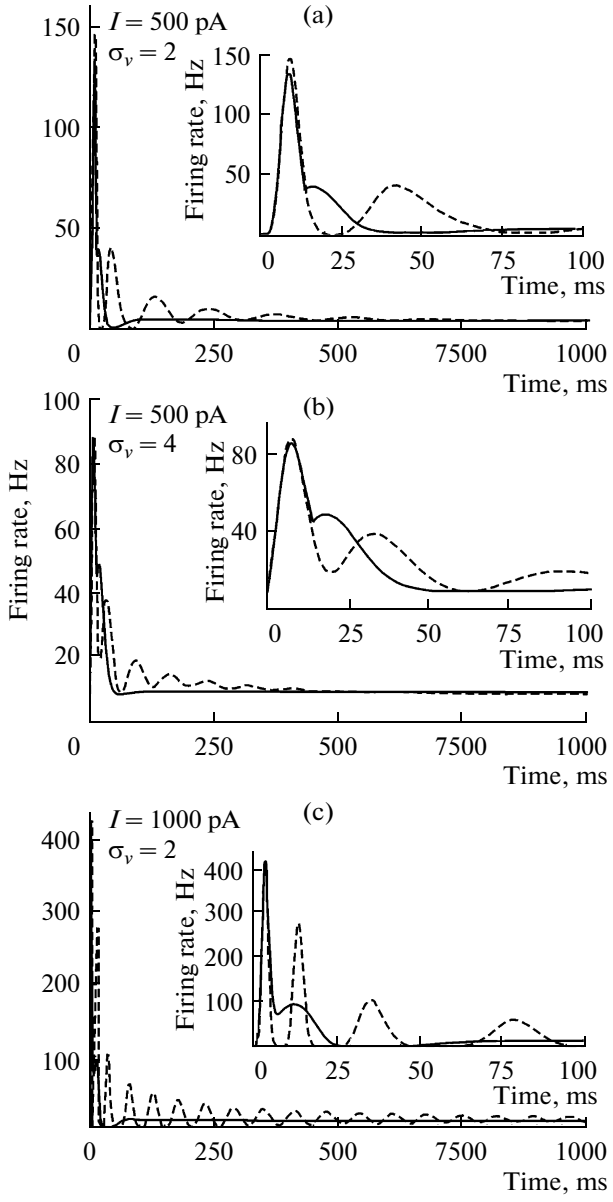

Fig. 4. Time course of the firing rate in the RD (dashed lines) and the FR (solid lines) models of a population of ALIF neurons at specified I and σ_V.

we take $N = 40$, $I_0 = 540$ μA/cm^2, $I_1 = 360$ μA/cm^2, $J_0 = 26$ μA/(Hz cm^2), $J_1 = 6.6$ μA/(Hz cm^2), other parameters as in p. 1.7.

A "stimulus line" oriented $\theta_0 = 0$ is presented for 100 ms, then its orientation is changed to $\theta_0 = \pi/4$. Figure 5 displays the reaction of the population ring to the presentation and the rotation of the stimulus. We can see that the $\theta_0 = 0$ stimulus elicits a response in the populations located near this direction, whereas upon rotation the bulk of activity shifts more than 45°, making a maximum about 60°. This is so because in the initial orientation the stimulus creates an angular distribution of the conductance of adaptive M-channels

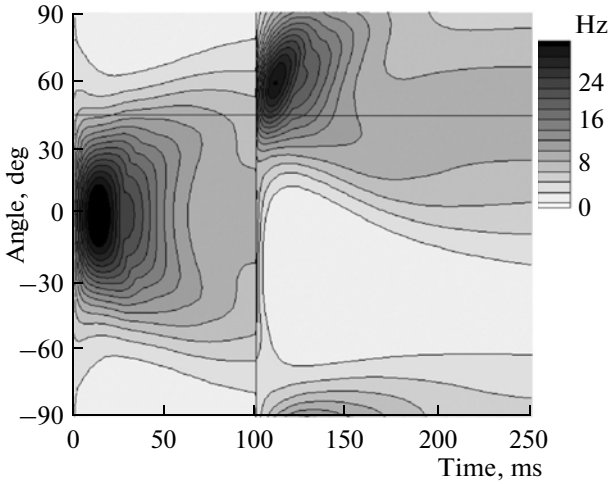

Fig. 5. Response of a ring of orientation-selective neuronal populations (distribution of firing rate $\nu(t, \theta)$) to a line stimulus of orientation 0° and to its rotation by 45° at $t =$ 100 ms. The shift of the activity peak by more than 45° corresponds to the psychophysical tilt after-effect.

that qualitatively reproduces the $\nu(t, \theta)$ distribution, shunting the activity in the vicinity of 45° more than at larger angles. Such model behavior reflects the real situation when a human subject, after having for some time looked at oblique lines, perceives vertical lines as inclined in the opposite direction (tilt after-effect). Detailed simulation of this effect is beyond the scope of the present paper.

DISCUSSION

Our model of a population of adaptive LIF neurons, comprising equations (34)–(37) with rate-dependent adaptive channel conductances (21), (22), is distinguished from the conventional FR models by that it reproduces the burst-like population activity evoked by rapidly rising excitation (volleys), as well as the decline of the firing rate under the influence of slow ion channels (spike adaptation). This is demonstrated by comparison with the full RD model. Admittedly, a spike-dependent model of adaptive conductance has been proposed by other authors [20]. The essential difference here is that in approximations (21), (22) we assume a non-instant rise in channel conductance, introducing the time constants τ^1_{AHP}, τ^1_M, thereby arriving at second-order ODEs rather than first-order ones. This adds accuracy to the ALIF- and especially to the FR model, and also obviates artifacts that might arise because the firing rate contains information on all neurons of the population (all realizations) but e.g. the earliest spikes preceding the population volley must not affect the adaptive conductances and first spikes of the "lagging" neurons: for this purpose, τ^1_{AHP} and τ^1_M provide the necessary

delays. Overall, the transition from the sophisticated RD to an FR model, i.e. to ODEs, affords computational simplicity at the expense of some loss of accuracy.

We have also demonstrated how the proposed FR model can be applied to interacting populations, with an example speculatively reproducing a known visual illusion. Here we based on a neuron model approximating the membrane potential and slow channel conductance. The mechanism considered here is perhaps just a part of adaptive processes giving rise to the tilt after-effect, e.g. synaptic ones; however, this can be a step toward more detailed simulation of the phenomenon.

We believe that the novel properties of the FR model would serve to improve the adequacy of large-scale models claiming to reproduce regimes with highly pronounced burst-like activity of neuronal populations under strong stimuli, as e.g. in epileptiform states. Thus, we can recommend this model for use in large-scale simulation of brain activity as well as for mathematical analysis of population models.

ACKNOWLEDGMENTS

The work was supported by the Russian Foundation for Basic Research (07-04-92167a, 09-01-00473a).

REFERENCES

1. P. Dayan and L. F. Abbott, *Theoretical Neuroscience* (MIT Press, Cambridge, Mass., 2002).
2. M. N. Zhadin, Biofizika **39** (1), 129 (1994).
3. O. Shriki, D. Hansel, and H. Sompolinsky, Neural Comp. **15**, 1809 (2003).
4. B. W. Knight, J. Gen. Physiol. **59**, 734 (1972).
5. A. Omurtag, B. W. Knight, and L. Sirovich, J. Comput. Neurosci. **8**, 51 (2000).
6. J. Eggert and J. L. van Hemmen, Neural Comp. **13**, 1923 (2001).
7. D. Nykamp and D. Tranchina, J. Comput. Neurosci. **8**, 19 (2000).
8. W. Gerstner and W. M. Kistler, *Spiking Neuron M odels:Single Neurons, Populations, Plasticity* (Cambridge University Press, Cambridge, 2002).
9. V. L. Dunin-Barkovskii, *Informational Processes in Neuronal Structures* (Nauka, Moscow, 1978) [in Russian].
10. A. V. Chizhov, L. J. Graham, and A. A. Turbin, Neurocomputing **70**, 252 (2006).
11. A. V. Chizhov and L. J. Graham, Phys. Rev. E **75**, 011924 (2007).
12. A. V. Chizhov and L. J. Graham, Phys. Rev. E **77**, 011910 (2008).
13. A. N. Pokrovskii, *Control Processes in Nerve Cells* (LGU, Leningrad, 1987) [in Russian].
14. A. V. Chizhov, S. Rodrigues, and J. R. Terry, Phys. Lett. A **369** (1–2), 31 (2007).
15. A. V. Chizhov and L. J. Graham,, in *Neuroinformatics–2007* (MIFI, Moscow, 2007), Pt. 3, pp. 17–24 [in Russian].
16. L. J. Borg-Graham, in *Cerebral cortex: Cortical models*, Ed. by P. S. Ulinsky, E. G. Jones, and A. Peters (Plenum Press, New York, 1998).
17. P. I. M. Johannesma, in *Neural Networks* (Springer, Berlin, 1968), pp.116–144.
18. D. Hansel and H. Sompolinsky, J. Comp. Neurosci. **3**, 7 (1996).
19. M. A. Webster, in *The Visual Neurosciences*, Ed. by L. M. Chalupa and J. S. Werner (MIT Press, Cambridge, Mass., 2004), pp. 936–947.
20. E. Muller, L. Buesing, J. Schemmel, and K. Meier, Neural Comp. **19**, 2958 (2007).